International Journal of Applied Engineering Research ISSN 0973-4562 Volume 13, Number 11 (2018) pp. 8871-8881

Analysis of Friction Systems on Shafts for Engineering Applications

Julián Esteban Herrera Benavides
Mechatronics Student, Department of Mechatronics Engineering, University Piloto of Colombia. Bogotá, Colombia.

Daniel Eduardo Espitia Corredor
Mechatronics Student, Department of Mechatronics Engineering, University Piloto of Colombia. Bogotá, Colombia.

Robinson Jimenez Moreno
Assistant Professor, Department of Mechatronics Engineering, Militar Nueva Granada University. Bogotá, Colombia.

Rubén Dario Hernández
Assistant Professor, Department of Mechatronics Engineering, University Piloto of Colombia.

David Herrera Alfonso
Assistant Professor, Department of Mechatronics Engineering, University Piloto of Colombia. Bogotá, Colombia.

Abstract
When a mechanism has been constructed that has a shaft supported in a circular compartment, without the presence of bearings or lubricants, the dry friction appears trying to prevent any rotational movement of it. This paper address a mathematical representation of mechanisms that deal with a static or dynamic situation under dry friction, in an analytical and computational way using MATLAB®. The objective is to expand the capacity of design of mechanical systems, improving the models that arise when handling shafts. Two equations are deduced and explained that compactly model the static and dynamic of this type of mechanism, allowing to analyze both phenomena at the same time. The analysis and development shown is valid only for shafts that do not accelerate translationally and also experience dry friction with the surface that supports them.

Keywords: Static dry friction, dynamic dry friction, transmissibility, imminent motion, transient response, MATLAB.

INTRODUCTION

When analyzing any mechanical structure that is in motion or not, it starts by creating a free-body diagram that shows adequately the forces that are acting, both in the composite body and in each link that conforms it [1]-[3] In this process it is necessary to know the supports and connections that exist, since these explain how the reaction is experienced by the body and therefore the forces that must be included in the free-body diagram.

Once the free-body diagram is obtained, analyzes can be made that allow the calculation of external forces that leave the system in a static, imminent motion and movement state. This step is important for applied engineering studies, since, in most mechanical systems applications, the torque of an engine that generates a movement in the mechanism must be argued. In order to expand the tools that fit this need through computational aids, basic concepts of the area literature are used for their contextualization, such as “Ingeniería Mecánica Estática” [4] and “Mecánica Vectorial para Ingenieros” [5]. Based on the dry friction [6]-[9] in shafts, to implement a simple method with which it can be determined the input to the system that generates the desired state.

If the desired state involves a movement, it means that the mechanism must overcome static friction [10]-[12] before experiencing acceleration. This situation, where it is moved from one state to another, is an analysis that has been covered by models called “Switching models” [13], which contemplate the effect of overcoming static friction.

In this way, works like the developed in [14], show the implementation of a mathematical model in which it includes functions that allow it to determine the direction of the force of the kinetic friction [15]-[19], but supposes that the magnitudes of the forces of static and kinetic friction are constant, i.e. that they are not affected by the different loads that the mechanism may be lifting.

On the other hand, the work presented in [20] shows the importance of keep present the friction force. The performance of a system depends totally of its mathematical model, a closer model to the real system allows to implement a better control [21]-[24] and therefore produce the expected results. Sometimes these results are simulated on Simulink [25]-[28].

In the present paper, an equation is developed with which the static and kinetic dry friction force can be analyzed taking into account that these depend on the inputs of the mechanism. This equation allows to create mathematical models [29]-[32], which, through software, can be simulated to obtain the total response of a mechanism, knowing that it must overcome the static friction before the movement.

The document is divided into five sections. Section 2 discusses the basic analysis to deduce an equation that expresses the steady state of a body supported on a shaft. Section 3 introduces the dynamic behavior with which the transient and stationary responses of the mechanism can be seen. This section takes into account that the friction can change direction depending on the direction of movement and the direction of entry of the system. In Section 4 it is analyzed problems that summarize the functionality of the two equations found and finally in section 5 the conclusions reached are presented.

STATIC ANALYSIS

The analysis of mechanical systems begins with knowing the type of support that is implemented to deduce the restrictions that the mechanism has. Figure 1 illustrates supports which, according to their nature, restrict the degrees of freedom of the system, these are related to contain any shaft that allows rotational movement.

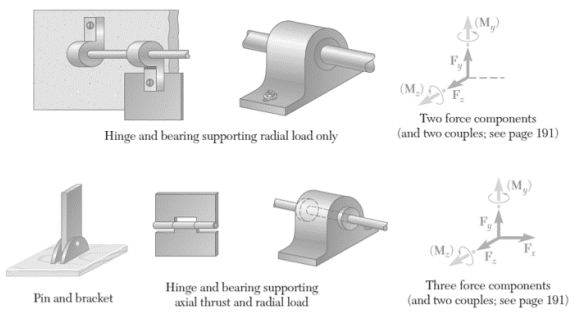

Figure 1. Supports and reactions involving shafts [5].

As noted in the images, restrictions are shown as vectors indicating the type of motion that cannot be generated. It can be seen that the rotation on the x-axis is free, something that is idealized. The present work focuses on examining this type of support considering that the restriction for a rotational movement in the x axis must exist, since dry friction is experienced, i.e. that the presence of lubricants is null or scarce and there is no resistance to the rolling since there are no balls that are rolling internally (bearings).

To begin to analyze a static situation the principles used of the mechanics are listed [5]:

- Parallelogram law for the addition of forces
- Principle of transferability
- Newton's Third Law, relate forces and momentum according to (1) and (2).

$$\mathbf{F} = m \cdot \mathbf{a} \tag{1}$$

$$\mathbf{M}_o = I \cdot \boldsymbol{\alpha} \tag{2}$$

Friction of Coulomb[33]:

Also known as dry friction, is the reaction that occurs between two surfaces that tend to slide without the presence of lubricants, the principles that describe the friction are:

1- It does not depend on the area in contact
2- The dry friction has a limit with respect to its magnitude that depends on the normal force and the nature of the surfaces in contact. The relationships are as follows.

When the system is in imminent motion:

$$F_f = N \cdot \mu_s \tag{3}$$

When the system is in motion:

$$F_f = N \cdot \mu_k \tag{4}$$

Once the maximum magnitude of the static friction force is exceeded, the kinetic friction is experienced, which is always smaller in magnitude, as shown in Figure 2.

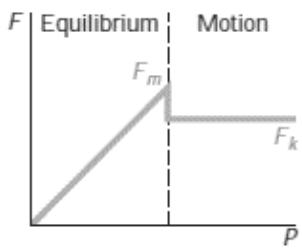

Figure 2. Behavior of dry friction [5].

By means of the above principles, the analysis of the machine that illustrates Figure 3, known as “Marble machine” [34], starts. Machine used as entertainment which has a transmission mechanism that is supported on a wooden shaft. The purpose of

this mechanism is to move marbles on roads in such a way that they are maintained in a cycle as long as the engine is energized.

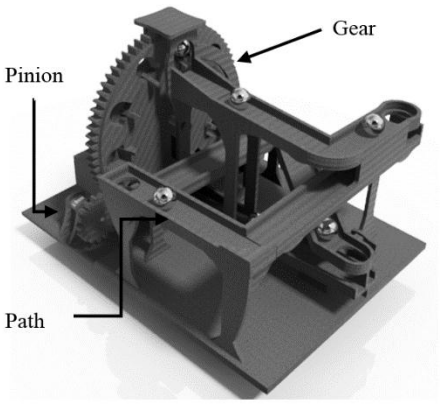

Figure 3. Parts of analyzed system. "Marble machine".

When the reduction motor is energized it generates a movement in the pinion and in the gear, but just before the movement is generated, the static friction must be overcome, however, what value should the input have to produce an imminent movement? Suppose the system is in an imminent motion situation.

In figure $4.a)$ the free body diagram of the gear is shown. In this it can be noticed the presence of the weight $\mathbf{W}_c$ and $\mathbf{W}_g$ of the marbles and the gear respectively, the force exerted by the pinion $\mathbf{F}_p$ and a reaction $\mathbf{R}$. The reaction $\mathbf{R}$ is a combination of the frictional force $\mathbf{F}_f$ and the normal force to the contact area $\mathbf{N}$ which occurs between the shaft and the gear. The reaction has been marked with a wavy line to specify that its rectangular components are the normal and the friction. The angle that forms between the normal and the reaction $\mathbf{R}$ is the "angle of friction" [5], and in the case of imminent movement this angle is symbolized as ϕ_s.

The friction angle is related to the coefficient of static friction as follows:

$$tan(\phi_s) = \mu_s \qquad (5)$$

The static friction radius r_s is shown in figure $4.b)$. This, regardless of the load situation of the system, will have the same magnitude in the shaft, and the line of action of the reaction $\mathbf{R}$ must pass through this circle in an imminent movement. The radius of friction is related by (6) to the radius of the shaft.

$$r_s = r \cdot sin(\phi_s) \qquad (6)$$

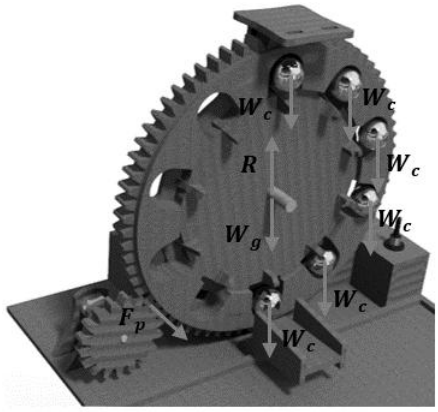

a) Forces acting on the gear

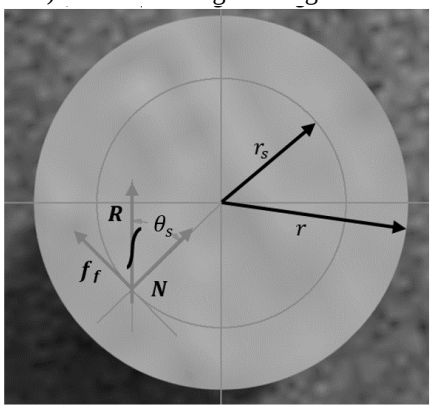

b) Reaction R, normal force, friction force, friction angle, radius and radius of friction.

Figure 4. System analyzed in imminent motion.

The important thing in Figure 4 is to look at the location in which the angle of friction with respect to the normal is and the relationship between the reaction $\mathbf{R}$ and the friction radius r_s in an imminent movement. The reaction $\mathbf{R}$ in this case prevents a translational and rotational movement, from the combination of the friction force $\mathbf{F}_f$ and the normal $\mathbf{N}$ since the shaft is not being transferred and the system is rotationally static.

With this being clear, a reference plane is inserted in the center of the gear and a momentum $\mathbf{M}$ is added in order to analyze the more general case of forces. The momentum represents one more input to the gear. Figure 5 shows the free-body diagram, in which the names of the entries have been ordered to give more clarity:

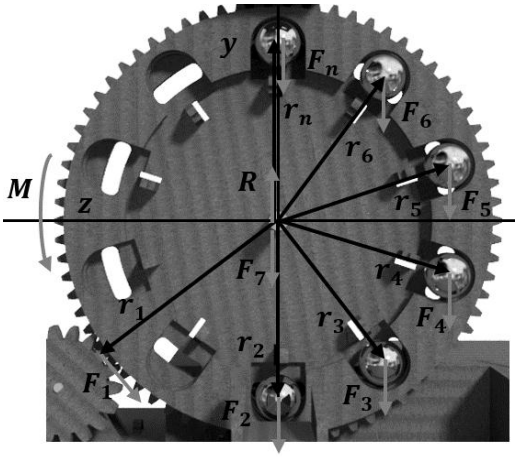

Figure 5. Free body diagram of the system analyzed.

The next step is to find an equivalent system of forces "force couple" [5] at the origin of the plane. For this, all the forces must be concurrent and apply the principle of the parallelogram for the addition of forces [5], then add all the momentum with respect to the origin and thus obtain the net force and the net pair.

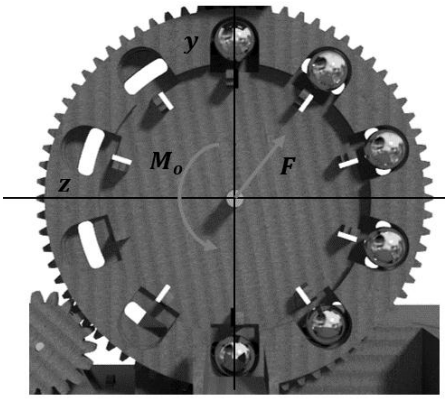

Figure 6. Free body diagram with "force couple" system

The equivalent force and the equivalent momentum are expressed from a vector sum, the graphical result of this step is shown in figure 6 and is related by (7) and (8).

$$\mathbf{F} = \mathbf{F}_1 + \mathbf{F}_2 + \mathbf{F}_3 + \mathbf{F}_4 + \mathbf{F}_5 + \mathbf{F}_6 + \mathbf{F}_7 + \mathbf{F}_n + \mathbf{R} \tag{7}$$

$$\mathbf{M}_o = \mathbf{M} + \mathbf{r}_1 \times \mathbf{F}_1 + \mathbf{r}_2 \times \mathbf{F}_2 + \mathbf{r}_3 \times \mathbf{F}_3 + \mathbf{r}_4 \times \mathbf{F}_4 + \mathbf{r}_5 \times \mathbf{F}_5 + \mathbf{r}_6 \times \mathbf{F}_6 + \mathbf{r}_7 \times \mathbf{F}_7 + \mathbf{r}_n \times \mathbf{F}_n + \mathbf{r} \times \mathbf{R} \tag{8}$$

The vector product used to find the momentum of reaction $\mathbf{R}$ includes the vector "$\mathbf{r}$", said force is located on the shaft of the gear as shown in figure 4.b).
By generality it is expressed the equation 7 and 8 as a summation, by (9) and (10).

$$\mathbf{F} = \sum_{i=1}^{n} \mathbf{F}_i + \mathbf{R} \tag{9}$$

$$\mathbf{M}_o = \mathbf{M} + \mathbf{r} \times \mathbf{R} + \sum_{i=1}^{n} \mathbf{r}_i \times \mathbf{F}_i \tag{10}$$

The forces being all coplanar produce a normal momentum to this plane that in this case is the plane $\mathbf{z}, \mathbf{y}$. This means that the equivalent momentum is on the "$\mathbf{x}$" axis and that the vector sum can only be expressed with scalars representing the magnitudes of each momentum vector. In other words, since all momentum vectors have the same direction, it is only necessary to evaluate the magnitudes of these to find the magnitude of the resulting momentum.
The magnitude of a momentum vector can be expressed by (11).

$$|\mathbf{M}_i| = \mathbf{r}_i \cdot \mathbf{F}_i \, sin(\theta_i) \tag{11}$$

So equation 10 can be written as (12) and (13).

$$M_o = M + r \cdot R sin(\phi_s) + \sum_{i=1}^{n} r_i \cdot F_i sin(\theta_i) \tag{12}$$

$$M_o = M + r_s \cdot R + \sum_{i=1}^{n} r_i \cdot F_i sin(\theta_i) \tag{13}$$

It can be seen that equation (13) uses the friction radius r_s to calculate the magnitude of the momentum exerted by the reaction $\mathbf{R}$. This is done since an imminent movement in the system is assumed, equation (6). If the resultant $\mathbf{F}$ is decomposed into its rectangular components, it can be stated that the magnitude of its components depends on the sum of the magnitudes of the components of the other forces (Eqs. 14 to 16).

$$F = \sqrt{F_z^{\,2} + F_y^{\,2}} \tag{14}$$

$$F_z = R_z + \sum_{i=1}^{n} F_{zi} \tag{15}$$

$$F_y = R_y + \sum_{i=1}^{n} F_{yi} \tag{16}$$

As it may be noticed, at this time no matter the actual direction of forces, it is simply assumed that all components are positive. In addition, although the images do not include a component in the z-axis for the force $\mathbf{R}$, it is being added in the equations to assume the more general case of forces.

Knowing the force and the net momentum, they are implemented the equations one and two, assuming an acceleration equal to zero, as seen in (17) to (19)

$$M_o = 0 = M + r_s \cdot R + \sum_{i=1}^{n} r_i \cdot F_i sin(\theta_i) = r_s \cdot R + M_{ex} \tag{17}$$

$$F_z = 0 = R_z + \sum_{i=1}^{n} F_{zi} = R_z + F_{ez} \tag{18}$$

$$F_y = 0 = R_y + \sum_{i=1}^{n} F_{yi} = R_y + F_{ey} \tag{19}$$

From equation 17 it can be obtained (20).

$$-r_s \cdot R = M + \sum_{i=1}^{n} r_i \cdot F_i sin(\theta_i) \tag{20}$$

Practically the equilibrium situation is almost fully described. From equations (18) and (19) it can be complemented the equation (20). Leading to the final result described by (22).

$$R = \sqrt{R_z^{\,2} + R_y^{\,2}} = \sqrt{\left(\sum_{i=1}^{n} F_{zi}\right)^2 + \left(\sum_{i=1}^{n} F_{yi}\right)^2} \tag{21}$$

$$\left(\sum_{i=1}^{n} F_{zi}\right)^2 + \left(\sum_{i=1}^{n} F_{yi}\right)^2 = \frac{\left(M + \sum_{i=1}^{n} r_i \cdot F_i sin(\theta_i)\right)^2}{r_s^{\,2}} \tag{22}$$

Using the relationship between the friction radius and the property of the contact surfaces μ_s, equations (5) and (6), it can be determined (23).

$$\left(\sum_{i=1}^{n} F_{zi}\right)^2 + \left(\sum_{i=1}^{n} F_{yi}\right)^2 = \frac{\left(M + \sum_{i=1}^{n} r_i \cdot F_i sin(\theta_i)\right)^2}{r^2 \cdot \frac{\mu_s^{\,2}}{\mu_s^{\,2} + 1}} \tag{23}$$

This equation expresses in a compact way the steady state of a body, which is supported by a shaft that experiences dry friction, due to sliding between the areas in contact.
To improve the presentation of the equation, the aggregate terms of equations (17), (18) and (19) are used, resulting in equation (24).

$$F_{ez}^{\,2} + F_{ey}^{\,2} = \frac{M_{ex}^{\,2}}{r^2 \cdot \frac{\mu_s^{\,2}}{\mu_s^{\,2} + 1}} \tag{24}$$

This equation facilitates the calculation of a momentum or some force that allows the system to move imminently. If the system is in motion simply needs to change the value of the static coefficient of friction by the kinetic μ_k, and the result obtained represents the minimum force or minimum momentum that must be exerted to maintain the movement. The terms ez, ey, ex have been used as a sub-index to remember that they represent the sum of external forces or momentum. In these terms, the reaction force $\mathbf{R}$ is not included as shown by equations (17), (18) and (19).

Now each term of this equation is explained.

$r \rightarrow$ Radio in which there is contact between the two rigid bodies and where friction is experienced.

$\mu_s \rightarrow$ Coefficient of static friction, this can be replaced by the kinetic μ_k.

$M_{ex} \rightarrow$ Magnitude of the momentum vector produced by all momentum and external forces without including $\mathbf{R}$, equation 17.

$F_{ez} \rightarrow$ Rectangular component directed through the z-axis of the resultant of all external forces without including $\mathbf{R}$, equation 18.

$F_{ey} \rightarrow$ Rectangular component directed through the y-axis of the resultant of all external forces without including $\mathbf{R}$, equation 19.

This equation must generate two results for the input, since it is possible to move the system in two directions, so it is necessary to pay attention to the negative values generated by the roots.

The importance of this result lies in the ease of solving a static problem without analyzing the magnitude and actual position of the frictional force. Simply put the forces of the system and solve the unknown of the equation. By means of this it is possible to argue the torque of an engine which can initiate a movement.

DYNAMIC ANALYSIS

If the rotational motion has already been generated at the momentum of overcoming static dry friction, it is time to evaluate the dynamic response of the system. For the following model it is assumed that equations 18 and 19 are still met, which means that the shaft is not experiencing translational acceleration. But since there is already a rotational acceleration, equation (17) must include that term, in addition the static radius of friction must be changed by the kinetic.

The variable ϕ in this case represents the angular displacement, I the opposition exerted by the body to rotate (Inertia) [35], according to (25) and (26).

$$M_o = I \cdot \alpha = r_k \cdot R + M_{ex} \tag{25}$$

$$I \cdot \frac{d^2\phi}{dt^2} = r_k \cdot \sqrt{F_{ez}{}^2 + F_{ey}{}^2} + M_{ex} \tag{26}$$

Equation (26), as it stands, has an error, suppose that the body moves positively in ϕ. If this occurs, the direction of the kinetic friction force must oppose this change and therefore the momentum of R must be negative, but if the direction of motion is opposite, the momentum of R must be positive. This means that there is a variant sign and is not being taken into account. For the above, the *sign()* function is used to determine the sign of a value. If the argument entered in the function is zero, it returns zero.

$$I \cdot \frac{d^2\phi}{dt^2} = -sign\left(\frac{d\phi}{dt}\right) \cdot r_k \cdot \sqrt{F_{ez}{}^2 + F_{ey}{}^2} + M_{ex} \tag{27}$$

The expression (27) takes into account the variations in the direction of motion and adjusts the direction of the momentum of the reaction R, but when the change is given in the direction of movement the static frictional force must be overcome. And this fact is not contemplated by the equation (27).

If equation (27) does not present acceleration and the body has no velocity, it follows that:

$$0 = -c \cdot \sqrt{F_{ez}{}^2 + F_{ey}{}^2} + M_{ex} \tag{28}$$

Notice that the *sign()* function has been removed and the kinetic friction radius has been changed by a constant " c ". The constant " c " represents all the radius values in which the reaction R can be located before reaching its maximum location r_s, which generates imminent movement. This equation expresses all the situations that occur before the imminent movement is generated.

The magnitude of all radii before imminent motion is:

$$|c| = \left| \frac{M_{ex}}{\sqrt{F_{ez}{}^2 + F_{ey}{}^2}} \right| \tag{29}$$

This radius can vary from 0 to r_s, if greater than this value, it means that the system begins to move and that therefore begins to rule equation 27. But the calculation of "$|c|$" only makes sense when the velocity is zero, since the body can be without acceleration but presenting velocity. If the body moves, there is no static dry friction.

The final step is to join these two situations, it is known that while there is movement, it must be used equation 27 and that when the radius $|c|$ is less or equal to r_s and there is no movement, it should not be met. The final result is as follows:

$$I \cdot \ddot{\phi} = \left(-sign(\dot{\phi}) \cdot r_k \cdot \sqrt{F_{ez}{}^2 + F_{ey}{}^2} + M_{ex}\right) \cdot sign\left(abs\left(sign\begin{pmatrix} sign\left(r_s - |c|\right) \\ -abs\left(sign\left(r_s - |c|\right)\right) \end{pmatrix}\right) + abs\left(sign\left(\dot{\phi}\right)\right)\right) \tag{30}$$

The expression *abs()* gives the absolute value of the argument that is entered. Equation 30 is a combination of equation 27 and a conditional created by functions *sign()* and *abs()*, said conditional ensures that equation 27 operates when the static friction has been overcome. To test equation 30, a case is assumed in which a force gradually increases to bring the system out of equilibrium and then gradually decrease until it returns to the initial state:

1- No movement, radius $|c|$ is between $0 \le |c| \le r_s$; $\dot{\theta} = 0$:

$$I \cdot \ddot{\phi} = \left(-sign(\dot{\phi}) \cdot r_k \cdot \sqrt{F_{ez}{}^2 + F_{ey}{}^2} + M_{ex}\right) \cdot sign\left(0 + 0\right) = 0 \tag{31}$$

2- The movement begins, $|c|$ is greater than r_s and the velocity is still zero, $|c| > r_s$; $\dot{\theta} = 0$:

$$I \cdot \ddot{\phi} = \left(-sign(\dot{\phi}) \cdot r_k \cdot \sqrt{F_{ez}{}^2 + F_{ey}{}^2} + M_{ex}\right) \cdot sign\left(1 + 0\right) \tag{32}$$

3- The body has speed and the force continues to increase, $|c|$ is greater than r_s and the velocity is different from zero, $|c| > r_s$; $\dot{\theta} \ne 0$:

$$I \cdot \ddot{\phi} = \left(-sign(\dot{\phi}) \cdot r_k \cdot \sqrt{F_{ez}{}^2 + F_{ey}{}^2} + M_{ex}\right) \cdot sign\left(1 + 1\right) \tag{33}$$

4- The body has speed and the force decreases, $|c|$ is less or equal to r_s and the velocity is different from zero. $0 \le |c| \le r_s$; $\dot{\theta} \ne 0$:

$$I \cdot \ddot{\phi} = \left(-sign(\dot{\phi}) \cdot r_k \cdot \sqrt{F_{ez}{}^2 + F_{ey}{}^2} + M_{ex}\right) \cdot sign\left(0 + 1\right) \tag{34}$$

5- The body has braked and the force continues to decrease, $|c|$ is less than r_s and the velocity is zero, $0 \le |c| < r_s;\ \dot{\theta} = 0$:

$$I \cdot \ddot{\phi} = \left(-sign(\dot{\phi}) \cdot r_k \cdot \sqrt{F_{ez}{}^2 + F_{ey}{}^2} + M_{ex}\right) \cdot sign\left(0+0\right) = 0 \qquad (35)$$

As has been observed, equation 30 should only work in cases 2, 3 and 4. If static friction has not been overcome, there has to be no acceleration or movement, and if there is movement, the value of the radius $|c|$ does not matter since if there is movement there is no static friction.

The solution of said differential equation represents the response of the system. Due to the complexity represented by this equation, Matlab [36]-[37] is used to graph the dynamic and static response of the system by means of a block diagram.

APPLICATION

As validation method is used a classic mechanics exercise reported in reference [5], using equation (24). Then, section a) of the exercise is chosen to analyze the transient response of the system (see problem solved 8.6 pg 363).

A pulley having a diameter of 101.6mm can be rotated about a fixed shaft having a diameter of 50.8mm, as seen in figure 7. The coefficient of static friction between the pulley and shaft is μ_s =0.2. Determine a) the minimum vertical force **P** required to start lifting a load of 2224.1N, b) the minimum vertical force **P** required to hold the load, c) the minimum horizontal force required to start lifting the same load.

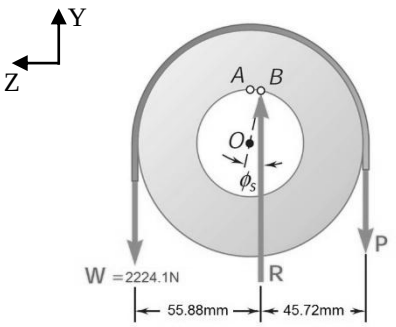

a)

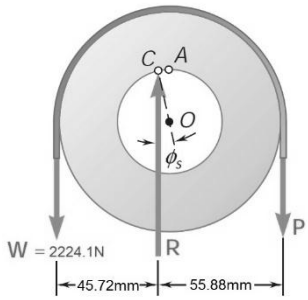

b)

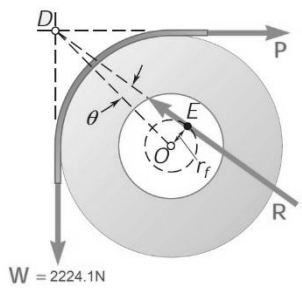

c)

Figure 7. Problem 6.6. Section a, b and c. [5].

When using equation (24), it is not necessary to know the location or magnitude of the frictional force, so the body diagrams of section "a" and "b" implement the equation in the same way. The z-axis is assumed to lie in the horizontal direction and the y-axis vertically according to the right-hand rule:

$$F_{ez} = 0 \qquad (36)$$

$$F_{ey} = -2224.1\text{N} - P \qquad (37)$$

$$M_{ex} = 2224.1\text{N} \cdot 50.8\text{mm} - P \cdot 50.8\text{mm} \qquad (38)$$

$$0^2 + (-2224.1\text{N} - P)^2 = \frac{M_{ex}{}^2}{(25.4\text{mm})^2 \cdot \frac{0.2^2}{0.2^2+1}} \qquad (39)$$

If P is solved, it can be obtained that:

$$P = \frac{2224.1\text{N}\left(50.8\text{mm} + \sqrt{645.16\text{mm}^2 \cdot \frac{0.2^2}{0.2^2+1}}\right)}{50.8\text{mm} - \sqrt{645.16\text{mm}^2 \cdot \frac{0.2^2}{0.2^2+1}}} \qquad (40)$$

In the expression found must be careful with the root, since it can generate a positive value and a negative value. It is therefore preferable to write the symbol ± in front of it.

$$P = \frac{2224.1\text{N}\left(50.8\text{mm} \pm \sqrt{645.16\text{mm}^2 \cdot \frac{0.2^2}{0.2^2+1}}\right)}{50.8\text{mm} - \left(\pm\sqrt{645.16\text{mm}^2 \cdot \frac{0.2^2}{0.2^2+1}}\right)} \qquad (41)$$

$$P = 2707.6\text{N}\ ;\ 1826.8\text{N} \qquad (42)$$

The reason why the root is not removed is because if the sign change is not taken into account, two values for P would never

have been found and these two values represent the magnitude of P that allows holding the load or lifting it. Clearly the magnitude of 1826.8N is the one that allows to hold it, since at that momentum the force of friction helps to hold it. While to move the load upwards it is necessary to make much more force by raising the load and overcoming the frictional force.

If one observes the exercise and the solution given in reference [5] it is evident that the procedure is more graphic since it is reasoned how the reaction in the arrow must act knowing the circle of friction.

Two responses were obtained as expected and each response obtained represents a situation where an imminent movement is generated for each direction.

For subsection c) the same procedure is followed and the following is obtained:

$$F_{ez} = -P \tag{43}$$

$$F_{ey} = -2224.1\text{N} \tag{44}$$

$$M_{ex} = 2224.1\text{N} \cdot 50.8\text{mm} - P \cdot 50.8\text{mm} \tag{45}$$

$$(-P)^2 + (-2224.1\text{N})^2 = \frac{M_{ex}{}^2}{(25.4\text{mm})^2 \cdot \dfrac{0.2^2}{0.2^2+1}} \tag{46}$$

$$\begin{aligned} &-638.7\text{mm}^2 P^2 + 2869.6\text{kN} \cdot \text{mm} P \\ &-3149\text{MN}^2 \cdot \text{mm}^2 = 0 \end{aligned} \tag{47}$$

This expression is related to a quadratic equation, resulting in the following:

$$P = 2556.34\text{N};\ 1935.02\text{N} \tag{48}$$

In order to analyze a dynamic situation, the system shown in figure 7.a) is again addressed, taking into account that there must now be a resistance to the movement exerted by the air to the pulley. It is assumed that the force P is an input that varies from 1832.6N to 3113.75N in less than a second, once it reaches its maximum value the force becomes a constant. The inertia of the pulley is $I = 1.355 kg \cdot m^2$. The coefficient of static and kinetic friction is $\mu_s = 0.2$ $\mu_k = 0.1$. The coefficient of viscous friction of the disc with air is $b = 1.355\text{N} \cdot \text{m} \cdot \text{s}$, so the torque due to the reaction of movement with air is $T_b = 1.355 \cdot \dot{\theta} \cdot \text{N} \cdot \text{m} \cdot \text{s}$. The external radius is $r_e = 50.8\text{mm}$ and the internal is $r = 25.4\text{mm}$.

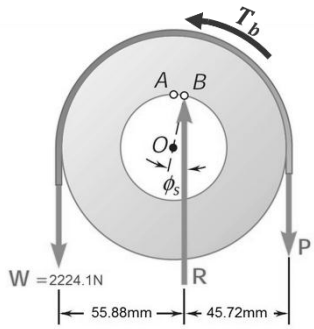

Figure 8. Dynamic situation.

Figure 8 represents the situation to be analyzed, the torque $\mathbf{T}_b$ has been added since there must be friction between the air and the pulley. The dynamic analysis is shown below.

Using equation 30 can solve this problem. The torque exerted by the air in the " M_{ex} " term of the equation must be taken into account. Next, the equation and its respective block diagram are presented:

$$\begin{aligned} I \cdot \ddot{\phi} = &\left(-sign(\dot{\phi}) \cdot r_k \cdot \sqrt{(W+P)^2} - b \cdot \dot{\phi} + P \cdot r_e - W \cdot r_e\right) \\ &\cdot sign\left(abs\left(sign\begin{pmatrix} sign\left(r_s - |c|\right) \\ -abs\left(sign\left(r_s - |c|\right)\right) \end{pmatrix}\right) + abs\left(sign\left(\dot{\phi}\right)\right)\right) \end{aligned} \tag{49}$$

$$r_s = r \cdot sin\left(tan^{-1}\left(\mu_s\right)\right) = 4.981\text{mm} \tag{50}$$

$$r_k = r \cdot sin\left(tan^{-1}\left(\mu_k\right)\right) = 2.527\text{mm} \tag{51}$$

$$|c| = \left| \frac{-b \cdot \dot{\theta} + P \cdot r_e - W \cdot r_e}{\sqrt{(W+P)^2}} \right| \tag{52}$$

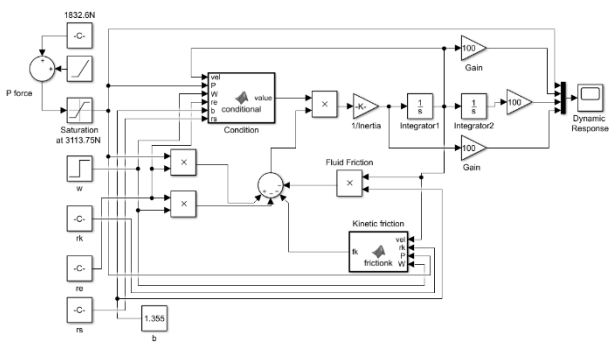

Figure 9. Block diagram of the dynamic problem.

The block diagram of Figure 9 summarizes the dynamic model of the system. There are two blocks that are responsible for calculating the conditional of equation 49 and kinetic friction. Note that the block diagram is nothing more than a mathematical model expressed in blocks to which is added a conditional that multiplies it. That result, according to equation 49, is equivalent to the inertia multiplied by the acceleration, so it is divided with the inertia to obtain the result of the acceleration. Then this result is integrated until the displacement is obtained. The displacement, velocity and acceleration have been multiplied by 100 to better show the result in the graph.

Remember that the units must be congruent N , m and rad/s. The newton strength holds the meter unit, so the mm should be converted to m.

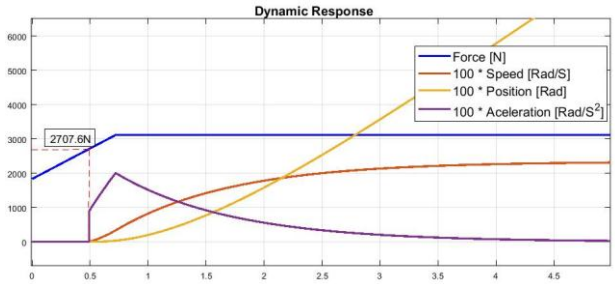

Figure 10. Dynamic system response.

In figure 10 the input is plotted in blue, the displacement in yellow, the speed in red and the acceleration in purple. Note that the force "P" starts at a value of 1832.6N, which means that the system must not move since the critical values are at 1826.8N and 2707.6N, any value in this range will not generate motion. Once the force exceeds the maximum critical value the system movement is generated, then the frictional force due to the fluid counteracts the torque that accelerates the mechanism causing it to stabilize. Note that the displacement ends up being a ramp and that the speed is a constant. So it is said that the system has stabilized, but when there is movement, there is no dry static friction.

The results obtained from the dynamic response are congruent with the statically calculated values. The advantage of using this method is that it allows to know more in depth values of all the variables that represent the system, besides it allows to simulate of a very real way a mechanism before constructing it, something useful to argue it.

Marble Machine

To conclude with the application section it is calculated the engine that should drive the mechanism of the Marble Machine.

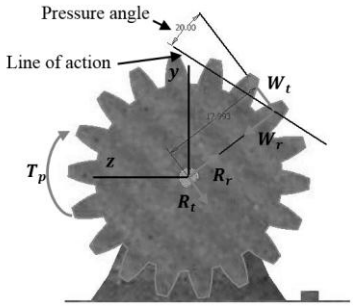

Figure 11. Free-Body Diagram of the Pinion

To begin with this problem, the free-body diagram of the pinion is analyzed as shown in figure 11. The pinion which has straight teeth has a pressure angle of 20° and the distance from the shaft to the pitch circle is 17.993 mm. The radial force $\mathbf{w}_r$ and the tangential $\mathbf{w}_t$ are the forces that occur when the teeth of the pinion and the gear come into contact, consequently, the reactions $\mathbf{R}_r$ and $\mathbf{R}_t$ occur. The momentum $\mathbf{T}_p$ is the torque being produced by the motor to bring the system into imminent motion, these terms can be analyzed in detail in reference [38].

From the theory of straight gears it is known that the forces $\mathbf{W}_r$ and $\mathbf{W}_t$ are perpendicular and their result passes through the line of action, so from the free-body diagram of the pinion it is obtained that:

$$T_p = W_t \cdot 17.993\text{mm} \tag{53}$$

$$W_r = W_t \cdot tan(20) \tag{54}$$

Now the free-body diagram of the gear is presented:

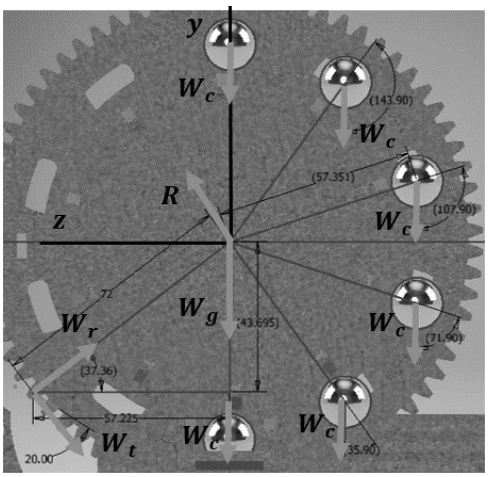

Figure 12. Free-body diagram of the gear.

The free body diagram has been created with the largest load situation on the shaft in mind, so the top marble is included and it is assumed that it has not left the compartment in the gear.
From Figure 12 it can be seen that all the marbles are at the same distance from the shaft and that by reaction at the point of

contact of the gear and the pinion the forces $\mathbf{w}_r$ and $\mathbf{w}_t$ are transmitted.

The diameter of the shaft is 6mm, the coefficient of static dry friction is $\mu_s = 0.5$, the weight of the marble is $W_c = 7\text{g} \cdot 9.81\text{m/s}^2$ and the weight of the gear is $W_g = 0.128\text{kg} \cdot 9.81\text{m/s}^2$. Using formula 24 it is obtained:

$$F_{ez} = -\frac{T_p}{20.07\text{mm}} \tag{55}$$

$$F_{ey} = -1.667\text{N} - \frac{T_p}{31.35\text{mm}} \tag{56}$$

$$M_{ex} = -12.12\text{N} \cdot \text{mm} + 4T_p \tag{57}$$

$$\left(-\frac{T_p}{20.07\text{mm}}\right)^2 + \left(-1.667\text{N} - \frac{T_p}{31.35\text{mm}}\right)^2 = \frac{\left(-12.12N \cdot \text{mm} + T_p \cdot 4\right)^2}{1.8\text{mm}^2} \tag{58}$$

Solving $\mathbf{T}_p$ it is obtained:

$$\mathbf{T}_p = 2.44\text{N} \cdot \text{mm} \ ; \ 3.631\text{N} \cdot \text{mm} \tag{59}$$

Once again it is gotten the torque to hold and lift the load. The solution reveals that a $37\text{gf} \cdot \text{cm}$ motor is required to operate the mechanism, which means that the $1.2\text{kgf} \cdot \text{cm}$ reducers that are on the market are ideal for this application. In addition, it is analyzed that the weight of the marbles will cause the gear to rotate clockwise as there is no motor, so the system is not self-blocking. This is deduced by the positive result obtained in the minimum torque to support the gear.

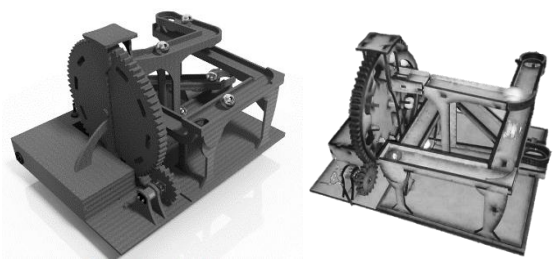

Figure 13. Marble Machine CAD and Marble Machine created.

CONCLUSIONS

It was possible to develop a methodology to analyze and model shafts subjected to dry friction, both in a static and dynamic situation. The results obtained when using the proposed methodology are not only congruent to those presented in the consulted bibliography, they complement them.

By means of the static deduction (equation 24) it is possible to solve problems involving dry friction in shafts without analyzing the magnitude, direction and orientation of the frictional force. This facilitates the calculation of inputs required to produce a movement in the mechanism.

From equation 30 it is possible to simulate the displacement of the system by evaluating the static and the dynamic at the same time, for this reason in the graphical answer of Figure 10 it is possible to know one of the results produced by the equation 24 with respect to the force P.

Discontinuous mathematical models such as equation 30 can be easily solved by block diagrams. Matlab, through Simulink, allows solving this type of systems without the need to implement mathematical methods that give the solution of the desired variable. As noted in the application section the most complex problem was the easiest to solve thanks to such software.

REFERENCES

[1] P. Felipe, C. Camilo, J. Robinson, Design of a Bio-Inspired Equine Robot Prototype, *International Review Of Mechanical Engineering ISSN: 1970-8734,* vol. 10, nº 1, pp. 12 - 17, 2016.

[2] C. Caceres, R. Jimenez, Modelado, discretización y control por realimentación de variables de estado de un sistema no lineal, *Clepsidra, ISSN: 1900-1355,* vol. 16, pp. 6 - 9, 2012.

[3] R. O. Oswaldo, R. J. Caipa y R. Luis, MODELING, DESIGN AND IMPLEMENTATION CONTROL OF SWING UP, *Revista Colombiana de,* vol. 1, nº 15, pp. 134-141, 2010.

[4] R. C. Hibbeler, *Ingeniería Mecánica Estática* (12th edition, Pearson, 2010).

[5] R. J. y. D. F. M. FERDINAND P.BEER, *Mecánica Vectorial para Ingenieros* (9th edition, Mc Graw Hill, 2010).

[6] A. Sören, S. Anders y S. Björklund, Friction models for sliding dry, boundary and mixed lubricated contacts, *Tribology International,* vol. 40, nº 4, pp. 580-587, 2007.

[7] O. Ben-David, G. Cohen y J. Fineberg, Short-time dynamics of frictional strength in dry friction, *Tribology Letters,* vol. 39, nº 3, pp. 235-245, 2010.

[8] N. Persson. B, O. Albohr, F. Mancosu, V. Peveri, N. Samoilov V y M. Sivebaek I, On the nature of the static friction, kinetic friction and creep, *Wear,* vol. 254, nº 9, pp. 835-851, 2003.

[9] A.-H. Brian, D. Pierre y D. W. C. Canudas, A survey of models, analysis tools and compensation methods for the control of machines with friction, *Automatica,* vol. 30, nº 7, pp. 1083-1138, 1994.

[10] R. Rober y M. M, Static and kinetic friction of rapeseed, *Research in Agricultural Engineering,* vol. 53, nº 1, pp. 14-19, 2007.

[11] A. Fall, B. Weber, M. Pakpour, N. Lenoir, N. Shahidzadeh, J. Fiscina, C. Wagner y D. Bonn, Sliding friction on wet and dry sand, *Physical Review Letters,* vol. 112, nº 17, pp. 175502-1 - 175502-4, 2014.

[12] H. Olsson, J. Åström. K, C. Canudas De Wit, M. Gäfvert y P. Lischinsk, Friction Models and Friction Compensation, *European Journal of Control,* vol. 4, nº 3, pp. 176-195, 1998.

[13] v. Campen, D. H. d. Kraker, A. v. d. Steen, L. Leine y R. Ingmar, Stick-Slip Vibrations Induced by Alternate Friction Models, *Nonlinear Dynamics,* vol. 16, pp. 41-54, 1998.

[14] R. C. FERNANDO, *Matlab Aplicado a Robótica y Mecatrónica*(1st,ALFAOMEGA, 2012).

[15] J. B. Peter, The significance and use of the friction coefficient, *Tribology International,* vol. 34, nº 9, pp. 585-591, 2001.

[16] K. Hashiguchi y S. Ozaki., Constitutive equation for friction with transition from static to kinetic friction and recovery of static friction, *International Journal of Plasticity,* vol. 24, nº 11, pp. 2102-2124, 2008.

[17] R. Ernest., The nature of the static and kinetic coefficients of friction, *Journal of Applied Physics,* vol. 22, nº 11, pp. 1373-1379, 1951.

[18] J. K. Horst, Kinetic friction locking for multi-body systems with friction, *ZAMP Zeitschrift für angewandte Mathematik und Physik,* vol. 46, nº 5, pp. 693-708, 1995.

[19] K. Nakano, Two dimensionless parameters controlling the occurrence of stick-slip motion in a 1-DOF system with Coulomb friction, *Tribology Letters,* vol. 24, nº 2, pp. 91-98, 2006.

[20] V. Ivan, F. Mária y K. Peter, Friction Effect Analysis of a DC Motor, *American Journal of Mechanical Engineering,* vol. 1, nº 1, pp. 1-5, 2013.

[21] T. Aleksei, G. E. A, P. Eduard, B. Juri, M. C. A y P. Ivo, Incorporation of fractional-order dynamics into an existing PI/PID DC motor control loop, *ISA Transactions,* vol. 60, pp. 262-273, 2016.

[22] E. Guerrero, J. Linares, E. Guzman, H. Sira, G. Guerrero y A. Martinez, DC Motor Speed Control through Parallel DC/DC Buck Converters, *IEEE Latin America Transactions,* vol. 15, nº 5, pp. 819-826, 2017.

[23] O. A. Saygın, Ç. Abdullah y T. Mustafa, Modeling And Position Control Of Scara Type 3D Printer, *INTERNATIONAL JOURNAL OF SCIENTIFIC & TECHNOLOGY RESEARCH,* vol. 5, nº 12, pp. 140-143, 2016.

[24] H. Ghariblu, A new mobile ball robot-dynamic modeling and simulation, *Applied Mathematical Modelling,* vol. 39, nº 10-11, pp. 3103-3115, 2015.

[25] H. Ehsan, Modeling and Simulation of Choppers Switching Via Matlab/Simulink, *International Journal of Intelligent Systems and Applications,* vol. 12, nº 1, pp. 1841-9267, 2015.

[26] E. van der Spoel, M. P. Rozing, Houwing-Duistermaat, J. J, P. Eline Slagboom, M. Beekman, A. J. M. de Craen, R. G. J. Westendorp y D. van Heemst, Modeling and Simulation of Systems Using MATLAB and Simulink, *Aging,* vol. 7, nº 11, pp. 956-963, 2015.

[27] M. Alexandru, The Modelling and Simulation of Bipolar Hybrid Stepping Motor by Matlab/Simulink, *Procedia Technology,* vol. 19, pp. 576-583, 2015.

[28] H. Sharma, N. Pal, Y. Singh y P. K. Sadhu, Development and Simulation of Stand Alone Photovoltaic Model Using Matlab/Simulink, *International Journal of Power Electronics and Drive Systems (IJPEDS),* vol. 6, nº 4, pp. 703-711, 2015.

[29] Y. L. Kuo, Mathematical modeling and analysis of the Delta robot with flexible links, *Computers and Mathematics with Applications,* vol. 71, nº 10, pp. 1973-1989, 2016.

[30] C. A. Radionova. L.V, Mathematical Model of the Vehicle in MATLAB Simulink, *Procedia Engineering,* vol. 129, pp. 825-831, 2015.

[31] D. Jullierme Emiliano Alves, P. Guilherme Augusto, Silva y P. Reinaldo Martinez, Longitudinal Model Identification and Velocity Control of an Autonomous Car, *IEEE Transactions on Intelligent Transportation Systems,* vol. 16, nº 2, pp. 776-786, 2015.

[32] A. S. Shah. Pritesh, Review of fractional PID controller, *Mechatronics,* vol. 38, pp. 29-41, 2016.

[33] H. D. y. R. A. F. YOUNG, *Física universitaria volumen 1*(13th edition, PEARSON EDUCACIÓN, 2012.)

[34] «Marble Machine,» [on line]. Available: https://marblemachine.org/. [last access: 5 07 2017].

[35] K. OGATA, *Dinaimca de Sistemas*(1st edition,PRENTICE-HALL, 1987.)

[36] L. Radionova y A. Chernyshev, Mathematical Model of the Vehicle in MATLAB Simulink, *Procedia Engineering,* vol. 129, pp. 825-831, 2015.

[37] X. H. Nguyen y M. P. Nguyen, Mathematical modeling of photovoltaic cell/module/arrays with tags in Matlab/Simulink, *Environmental Systems Research,* vol. 4, nº 1, p. 24, 2015.

[38] R. L. Norton, *Diseño de Máquinas un enfoque integardo*(4th edition, prentice Hall, 2011).